BEAM TRACING FOR FAST RCS PREDICTION OF ELECTRICALLY LARGE TARGETS

H.-G. Park, H.-T. Kim, and K.-T. Kim[*]

Department of Electrical Engineering, Pohang University of Science & Technology, San 31, Hyojadong, Namgu, Pohang, Kyungbuk 790-784, Korea

Abstract—A new radar cross section (RCS) prediction technique based on beam tracing is presented. The incident plane wave is modeled as a set of trigonal ray tubes, and each ray tube is traced and recursively subdivided as its reflection aspect. The calculation time of the proposed method is independent of target size. The proposed method provides accurate solutions and is efficient for RCS analysis of electrically large targets.

1. INTRODUCTION

The shooting and bouncing rays (SBR) method is widely used to calculate the radar cross section (RCS) of targets, and it provides accurate results for targets that have multiple reflections. However, SBR requires a huge calculation time for electrically large targets because the results converge only if the density of the incident ray tubes is greater than ten rays per wavelength [1] and because its calculation time is proportional to the number of incident ray tubes.

The calculation time of SBR depends on two factors: the number of incident ray tubes and the number of intersection tests per ray tube. To decrease the number of incident ray tubes, the multiresolution grid algorithm in SBR (MSBR) was proposed [2, 3]. MSBR represents the incident plane wave by a set of ray tubes that have a relatively larger cross section than in the conventional SBR. Although MSBR has a constraint that the incident ray tubes should be smaller than the smallest facet of the target to guarantee accuracy, MSBR provides an efficient RCS prediction because the smallest facet is commonly much larger than the grid of the conventional SBR.

To decrease the number of intersection tests per ray tube, space division algorithms and angular division algorithms have been applied to the ray tracing procedure of SBR. In the conventional SBR, the intersection tests should be performed with all facets of the target for each ray tube, which causes a huge computation cost. However, the number of intersection tests and the calculation time of SBR can be reduced by using octree structures, a space division algorithm, or the distribution information table derived using an angular division algorithm [4–6].

In this paper, we propose a new RCS prediction method based on beam tracing [7]. The proposed beam tracing has a significantly shorter computation time, especially for electrically large targets, than the conventional SBR. This benefit comes from the fact that the proposed method can decrease the number of incident ray tubes significantly, rather than the number of intersection tests per ray tube. The conventional SBR represents the incident plane wave by a dense rectangular grid of ray tubes, each of which is traced as it reflects from the target without subdivision. The proposed method, however, models the incident plane wave as a set of trigonal ray tubes whose cross sections are the directly shown partitions of the facets, and each ray tube is traced and recursively subdivided as it reflects from the target. Targets analyzed in this paper are modeled as a set of planar triangles because the proposed method has a similar motivation to MSBR in that adjacent incident ray tubes which have the same reflection path can be merged without loss of accuracy in RCS analysis.

Unlike the conventional SBR and MSBR, the proposed method is based on beam tracing and results in a computation cost that is independent of the electrical size of the target. The calculation time of the proposed method only depends on the number of facets that construct the target, so the proposed method can be very efficient for electrically large targets such as naval vessels at X-band frequencies.

2. METHOD

The proposed method consists of two steps: beam generation and beam tracing. To increase efficiency, incident ray tubes are only generated for the directly-visible components of the target, and to simplify subsequent procedures all ray tubes have trigonal cross sections. For example, consider a simple target modeled using a collection of triangular facets (Figure 1). Conventional SBR represents the incident plane wave as $11 \times 12 = 132$ ray tubes, but the proposed method only requires six ray tubes (Figure 2).

Beam generation procedure is as follows:
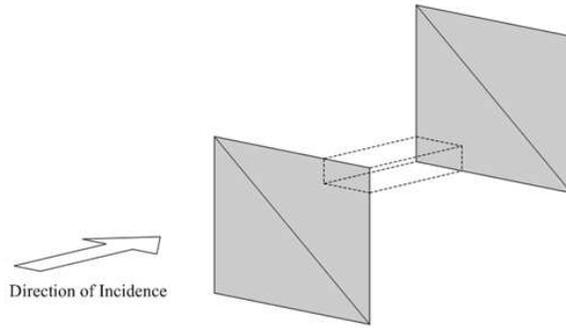
Figure 1. Two quadrangles that partially overlap (ends of rectangular prism).
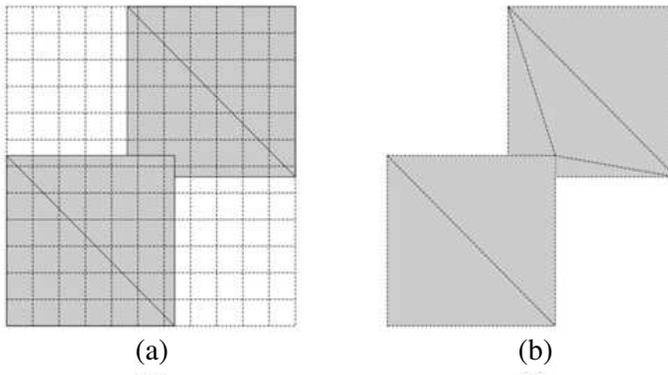
Figure 2. Incident ray tube grid: (a) conventional SBR and (b) proposed method.

1) Transform the coordinate system of the target into the Initially Incident Beam (IIB) coordinate system, where the direction of the incident wave is defined as the $-\hat{z}$ direction.

2) Calculate an orthogonal projection onto the incident plane for every facet that the incident wave hits. In the IIB coordinate system, the orthogonal projection is obtained by simply removing the z-coordinates of vertices.

3) Perform 2D polygon clipping [7, 8] according to the depth order of facets: a polygon projected from a facet farther from the beam source is clipped by nearer polygons.

4) Divide the remaining polygons into the smallest possible number of triangles [9]. This simplifies subsequent procedures by making all beams trigonal.

Each triangle is an initial grid which corresponds roughly to the grid of the conventional SBR method, and the initial trigonal beam transmitted from the grid hits only one facet.

The initial beams reflect off the surfaces that they hit. When the reflected beam hits a portion of the target's surface that consists of several facets, the beam should be subdivided because it is reflected in numerous directions depending on the orientations of the facets. The beam tracing step performs these subdivisions and subsequent tracing processes recursively for all initial beams sequentially. The beam tracing procedure for each initial beam can be described as follows:

1) Calculate the direction of the reflected beam.

2) Calculate the orthogonal projections of facets that face the reflected beam after transforming the coordinate system into the Reflected Beam coordinate system to redefine the direction of the reflected beam to be $-\hat{z}$.

3) Apply the hidden surface algorithm [8] to projected polygons according to the depth order of facets: a polygon projected from the facet farther from the reflected beam source is clipped by nearer polygons.

4) Find the intersections between the reflected beam and the projected polygons in a 2D plane.

5) Find portions of the beam which do not hit any facet by subtracting the beam-polygon intersections from the orthogonal projection of the beam.

6) Divide the intersections into the smallest possible number of triangles [9]. Each triangle is the cross section of the next-order reflected beam.

This beam division process is performed recursively for next-order reflected beams and the beam tree [7] is constructed to describe the reflection aspect of each initial beam. The root node of the beam tree is the first-order reflected beam. The beam tree proposed in this paper has two kinds of child nodes, those that originate from facets hit by the beam (intersected child nodes) and those that originate from facets that are not (non-intersected child nodes). Intersected child nodes at the ith level correspond to the ith-order reflected beams and will have child nodes. Non-intersected child nodes represent the portion of the parent beam which does not reflect from any facet; they are leaf nodes.

(a)

(b)
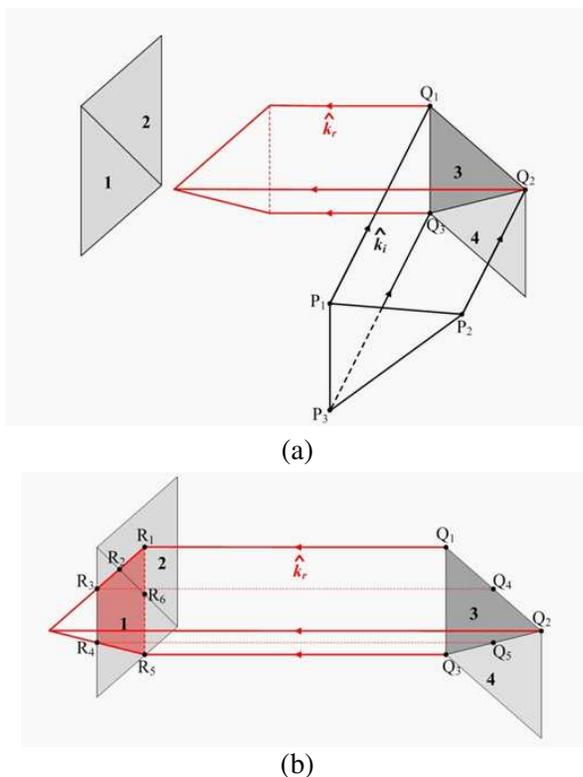
Figure 3. Geometry of the reflection: (a) first-order reflection, (b) second-order reflection. Initial trigonal grid $P_1P_2P_3$ is orthogonal to $\hat{k}_i$. Triangular facets are labeled with index numbers. In the initially incident beam coordinate system, $\hat{k}_i$ is equivalent to $-\hat{z}$.

For example (Figure 3), for the initial trigonal grid $P_1P_2P_3$, the root node is the first-order reflected beam whose direction vector is $\hat{k}_r$ and cross section is the triangle $Q_1Q_2Q_3$. The second level consists of five child nodes (Figure 4). The leftmost node $R_1R_2R_6$ denotes the second-order reflected beam whose cross section is $R_1R_2R_6$, the intersection between the parent beam and the facet labeled 2. The rightmost node $Q_2Q_4Q_5$ corresponds to the portion of the first-order reflected beam which does not reflect any facet. Every child node of the beam tree stores the reflection history which records which patches have reflected the beam and the coordinates of its three vertices in the IIB coordinate system.

For all non-intersected child nodes, the physical optics integral [10]
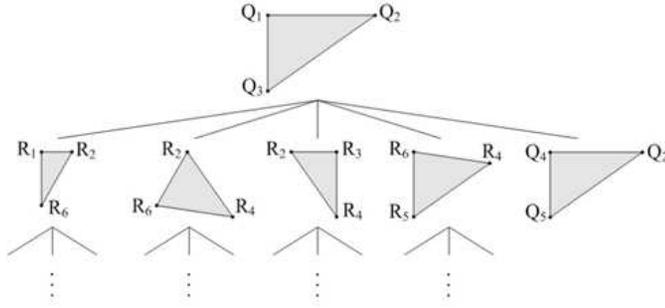
Figure 4. A representation of the beam tree to describe the reflection aspect. Triangle designations correspond to those in Figure 3. In this paper, maximum tree depth was set to five.
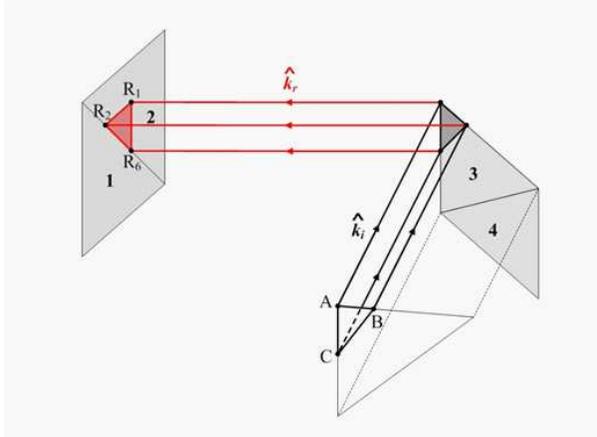
Figure 5. A virtual grid for the non-intersected child node, $R_1R_2R_6$.

is performed to obtain the scattered field of the target. For example, if the reflected beam from $R_1R_2R_6$ does not hit any facet, $R_1R_2R_6$ is a non-intersected child node at the third level of the tree and its scattered field is calculated by performing the physical optics integral on the exit position. A virtual grid, ABC, on the incident plane can be assumed by inverse-tracing (Figure 5), and the incident ray beam transmitted from this virtual grid reflects one planar facet at each reflection stage. Therefore, the output ray tube does not spread through the reflection process and is uniformly dispersed on the exit position. The proposed method can satisfy the linear-phase-variation approximation [1], although relatively large ray beams are used.

3. RESULTS

The warship model in Figure 6 was employed to demonstrate the proposed method. In order to investigate the computational efficiency, the target in Figure 6 was magnified to 5, 10, 15, or 25 times its actual size. All five targets with different sizes were modeled with 482 triangular facets. The monostatic RCS of the five targets has been computed in the azimuth and elevation planes as illustrated in Figure 7, at a frequency of 10 GHz.

In Figure 8, the number of incident ray tubes needed to calculate the monostatic RCS were measured for the proposed method and conventional SBR. For the conventional SBR, the number of incident ray tubes varies with the visible area of the target as the incident
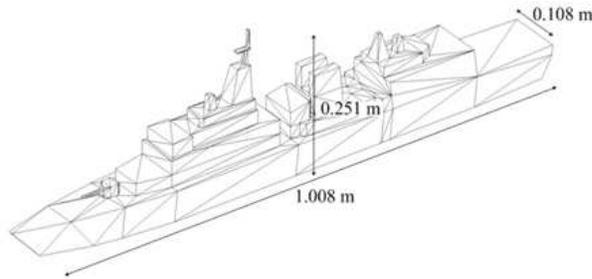
Figure 6. Dimensions and facets of the warship model used in simulations: The number of facets is 482.
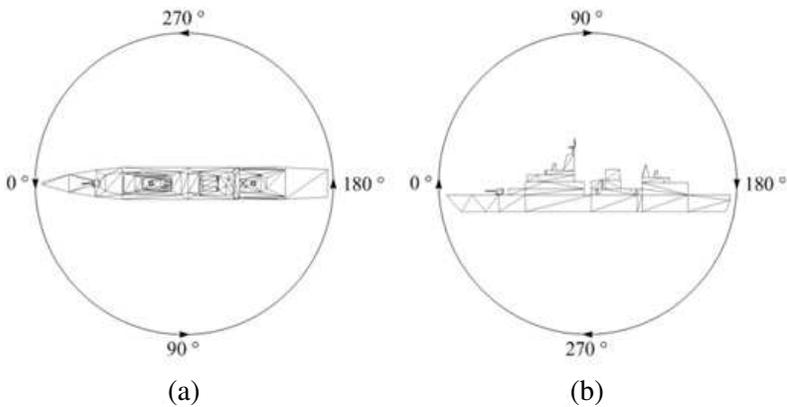
Figure 7. Angle planes: (a) azimuth plane and (b) elevation plane.
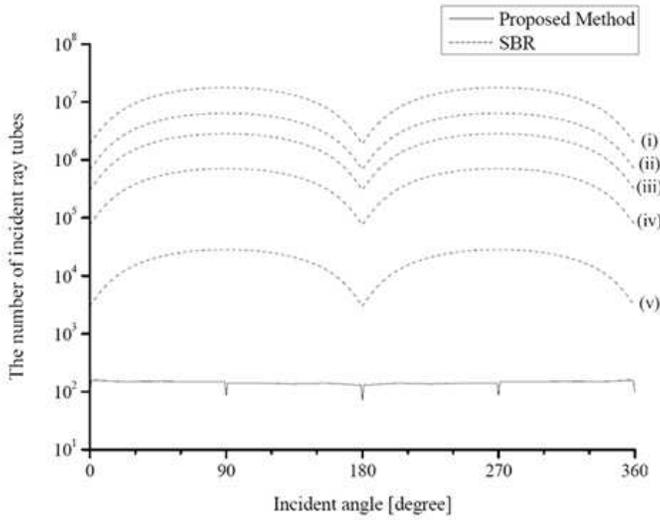
(a)
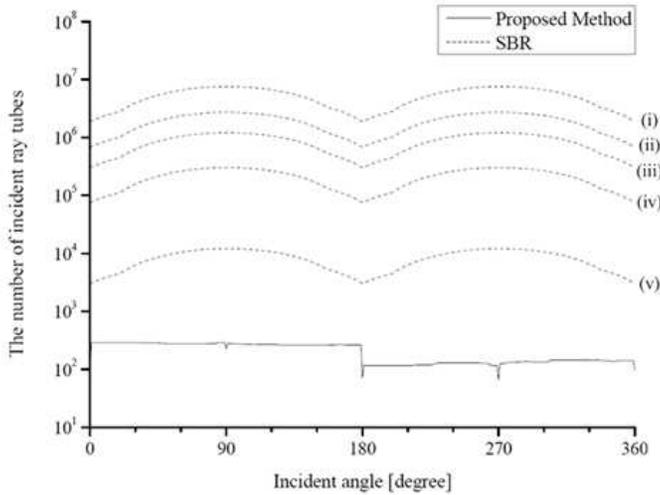
(b)

Figure 8. The number of incident ray tubes: (a) azimuth plane and (b) elevation plane. (i) SBR with 25 times magnified target. (ii) SBR with 15 times magnified target. (iii) SBR with 10 times magnified target. (iv) SBR with 5 times magnified target. (v) SBR with the target in Figure 6.
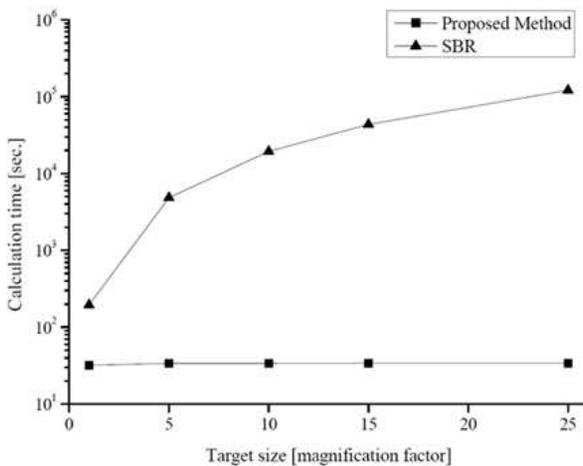
(a)
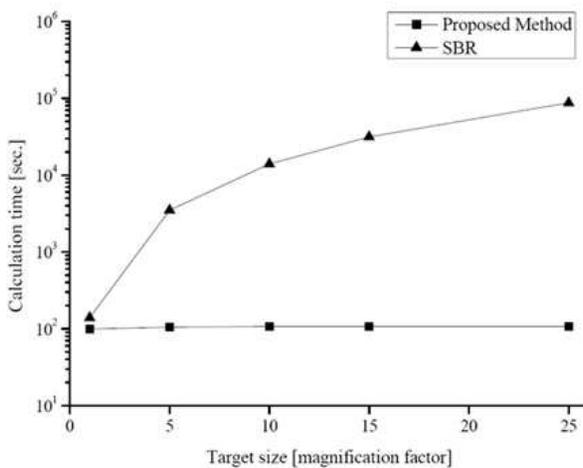
(b)

Figure 9. Computation time vs. the size of the target: (a) azimuth plane and (b) elevation plane.

angle is changed, whereas it varies with the number of visible facets for the proposed method. Because the size of the incident ray tube is chosen as a tenth length of the wavelength in the conventional SBR, the number of incident ray tubes of SBR increases rapidly as the target size increases and is thus directly proportional to the

square of the magnification factor, as shown in Figure 8. However, as aforementioned, the proposed method is independent of the target size and is dependent only on the number of visible facets. In general, electrically large targets can be modeled with facets whose sizes are much larger than the conventional SBR grid size. This implies that the number of visible facets for the proposed beam tracing is much smaller than the number of grids for the conventional SBR. Because the proposed method uses a number of incident ray tubes directly proportional to the number of visible facets, it can be significantly less than that of the conventional SBR.

In Figure 9, the computation times required by the proposed method and conventional SBR to calculate the RCS are compared in terms of target size. Clearly, the increase of the computation time for the conventional SBR is proportional to the square of target sizes. However, it is independent of target size and maintains a very small value with the proposed method. It should be noted that the subdivision of ray tubes in the beam tracing of the proposed method may increase the computational complexity. However, its effect on the total computational time is much less than the number of incident ray tubes, especially for electrically large targets.

To demonstrate the relation between the computation time and the number of facets modeling the target, the warship model in Figure 6 was magnified to 5 and 10 times its size. In addition, each magnified target as well as the original target has been modeled by 482, 918, 1496, 2086, 3724, 6777, and 9887 facets. The elapsed times to calculate the monostatic RCS of the conventional SBR and the proposed beam tracing are compared in Figure 10. Clearly, the elapsed time of the proposed method increases with the number of modeled facets, but it is independent of the target size. In contrast, the computation time of the conventional SBR dramatically increases with the target size rather than the number of facets. This is because the elapsed time of the conventional SBR is linearly proportional to the number of facets, and square of the target size. As the target size increases and the number of facets decreases, the proposed method is more efficient than the conventional SBR. However, the proposed beam tracing may be inefficient for complex and relatively small targets. For example, the proposed method requires more calculation time than conventional SBR for the unmagnified targets modeled with many facets in Figure 10. The proposed method is suitable for complex targets only when their electrical sizes are large enough. In summary, the proposed method has a pronounced improvement in computational efficiency over the conventional SBR when the target size, rather than the number of modeled facets, increases. It should be noted that
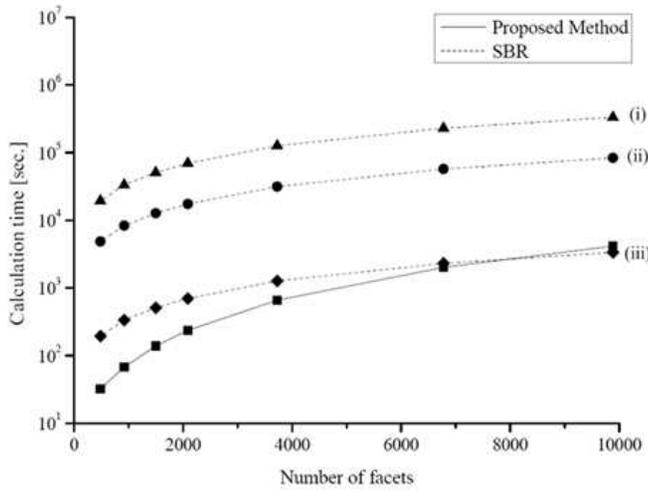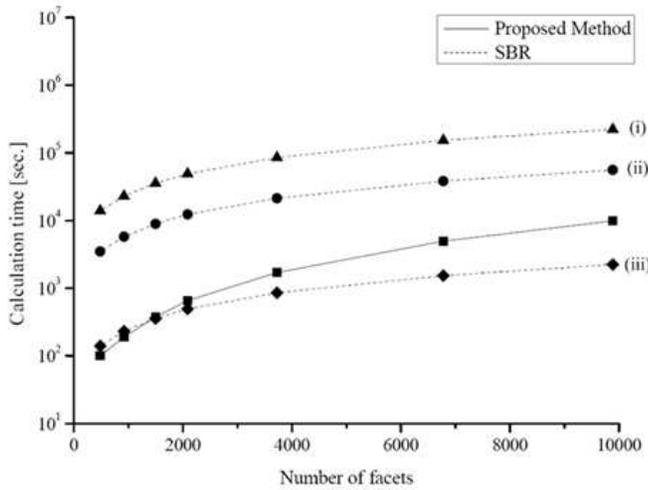
Figure 10. Computation time vs. the number of facets: (a) azimuth plane and (b) elevation plane. (i) SBR with 10 times magnified targets. (ii) SBR with 5 times magnified targets. (iii) SBR with unmagnified targets.

(a)

(b)
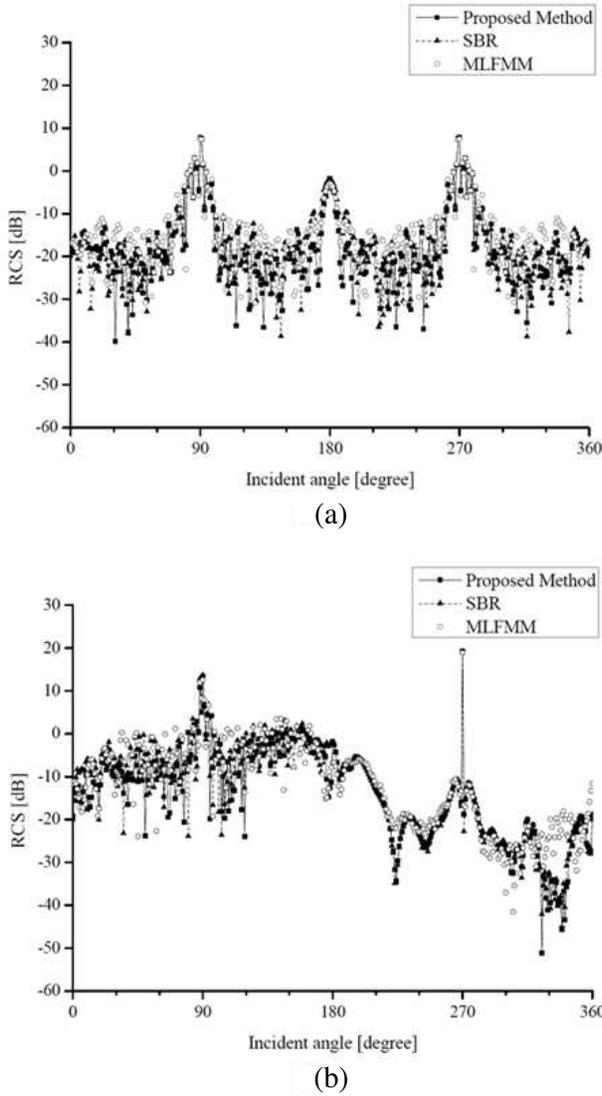
Figure 11. Monostatic RCS of the warship model: (a) azimuth plane and (b) elevation plane.

the conventional SBR has estimated elapsed times to calculate the monostatic RCS of up to about 387 and 258 days with the 100 times enlarged target having 9887 facets in the azimuth and elevation plane, respectively, whereas the beam tracing maintains the same times as in Figure 10.

The monostatic RCS of the target model in Figure 6 calculated with the proposed method is presented in Figure 11, and its accuracy is compared with those of the conventional SBR and the method of moments (MoM). The results from the MoM have been obtained by the multilevel fast multipole method (MLFMM) of the commercial FEKO software [11]. In Figure 11, the RCS of the proposed method exhibits good agreement with those of the conventional SBR and MLFMM. Of course, there is a small amount of difference in RCS between the beam tracing and the conventional SBR. This is attributed the fact that the modeling difference of the incident plane wave between the two methods, as shown in Figure 2. The relative RMS error between the proposed method and conventional SBR is very low: 4.36 dB and 3.72 dB in the azimuth and elevation plane respectively. In addition, the RMS error between the proposed method and the MLFMM are 6.11 dB and 6.16 dB, while those between the conventional SBR and the MLFMM are 6.15 dB and 5.81 dB. This implies that the proposed method and the conventional SBR show similar performance in terms of RCS prediction accuracy.

4. CONCLUSION

We have proposed a fast RCS prediction method for electrically large targets. The proposed method is based on the beam tracing principle. This leads the computation time to be independent of the electrical size of targets. It has been verified that the method is as accurate as the conventional SBR, while computational complexity is much less, especially for electrically large targets The proposed method is an attractive alternative to the conventional SBR due to its fast computation speed with relatively accurate RCS prediction.

ACKNOWLEDGMENT

REFERENCES

1. Ling, H., R. C. Chou, and S. W. Lee, "Shooting and bouncing rays: calculating the RCS of an arbitrarily shaped cavity," *IEEE Trans. on Antennas Propag.*, Vol. 37, No. 2, 194–205, 1989.
2. Suk, S.-H., T.-I. Seo, H.-S. Park, and H.-T. Kim, "Multiresolution grid algorithm in the SBR and its application to the RCS calculation," *Microw. Opt. Tech. Lett.*, Vol. 29, No. 6, 394–397, 2001.

3. Gao, P. C., Y.-B. Tao, and H. Lin, "Fast RCS prediction using multiresolution shooting and bouncing ray method on the GPU," *Progress In Electromagnetics Research*, Vol. 107, 187–202, 2010.

4. Jin, K.-S., T.-I. Suh, S.-H. Suk, B.-C. Kim, and H.-T. Kim, "Fast ray tracing using a space-division algorithm for RCS prediction," *Journal of Electromagnetic Waves and Applications*, Vol. 20, No. 1, 119–126, 2006.

5. Kim, B.-C., K.-K. Park, and H.-T. Kim, "Efficient RCS prediction method using angular division algorithm," *Journal of Electromagnetic Waves and Applications*, Vol. 23, No. 1, 65–74, 2009.

6. Park, K.-K. and H.-T. Kim, "RCS prediction acceleration and reduction of table size for the angular division algorithm," *Journal of Electromagnetic Waves and Applications*, Vol. 23, Nos. 11–12, 1657–1664, 2009.

7. Heckbert, P. S. and P. Hanrdahan, "Beam tracing polygonal objects," *Computer Graphics (Proc. SIGGRAPH)*, Vol. 18, No. 3, 119–127, 1984.

8. Weiler, K. and P. Arherton, "Hidden surface removal using polygon area sorting," *Computer Graphics (Proc. SIGGRAPH)*, Vol. 11, No. 2, 214–222, 1977.

9. De Berg, M., M. Van Kreveld, M. Overmars, and O. Schwarzkopf, *Computational Geometry*, Springer, 2000.

10. Klement, D., J. Preissner, and V. Stein, "Special problems in applying the physical optics method for backscatter computation of complicated objects," *IEEE Trans. on Antennas Propag.*, Vol. 36, No. 2, 228–237, 1988.

11. FEKO Suite 5.5, EM Software and Systems. Available: http://www.feko.info/.